MICROSTRUCTURAL CHANGES OF ODS FERRITIC STEEL POWDERS DURING MECHANICAL ALLOYING

Zbigniew OKSIUTA*

*Zakład Inżynierii Materiałowej i Biomedycznej, Wydział Mechaniczny, Politechnika Białostocka,
ul. Wiejska 45 C, 15-351 Białystok

oksiuta@pb.edu.pl

Abstract: The ODS ferritic steel powder with chemical composition of Fe-14Cr-2W-0.3Ti-0.3Y2O3 was mechanically alloyed (MA) either from elemental or pre-alloyed powders in a planetary ball mill. Different milling parameters have been used to investigate their influence on the morphology and microstructure of the ODS ferritic steel powder. The time of MA was optimized by studying the structural evolution of the powder by means of X-ray diffractometry and TEM. In the case of elemental powder very small, about 10 µm in diameter, spherical particles with a large surface area have been obtained. Flakey-like particles with an average size of about 45 µm were obtained in the case of the pre-alloyed powder. The lattice strain calculated from XRD spectra of the elemental and pre-alloyed powders exhibits a value of about 0.51 % and 0.67, respectively. The pre-alloyed powder after consolidation process showed the highest density and microhardness value.

1. INTRODUCTION

30 years have passed since Benjamin (1970) used a mechanical alloying (MA) technique for the first time to synthesize different kinds of materials. The structural and chemical changes during MA in a solid state powder are so complex that it is difficult to predict particular reaction or time needed to obtain final product properties. The MA process is commonly used to obtain intermetallic powders starting from elemental powder particles and it is one of the most popular methods for the production of oxide dispersion strengthening (ODS) ferritic steel reinforced with yttrium oxide (Y_2O_3). ODS ferritic steel is candidate material for structural applications in future fusion reactors, due to their excellent high temperature properties, thermal stability and irradiation resistance. Such material can be produced using various initial powders, e.g., elemental and/or pre-alloyed powders as well as milling devices and MA parameters (Suryanarayana, 2001).

The physical and chemical features of the mechanically alloyed powders depend on the MA parameters, such as: type of ball milling device, linear velocity, type, size and number of the balls, the balls-to-powder weight ratio (BPR), the milling atmosphere, a process control agent (PCA), process temperature and many others (Suryanarayana, 2001; Mukhopadhyay et al., 1998; Cayron et al., 2004; Chul-Jin, 2000; Ohtsuka et al., 2005; Patil et al., 2005). In spite of plenty of published articles there is still a lack of systematic studies comparing morphology, size distribution and other characteristics of ODS ferritic steel powders produced by ball milling method.

In this paper the microstructural evolution of elemental and pre-alloyed ODS ferritic steel powders during MA in a planetary ball mill has been studied to obtain the desired solid solution properties. Different ball milling conditions were investigated to establish their influence on the morphology and microstructural changes of the ODS ferritic steel powders.

2. EXPERIMENTAL PROCEDURE

Selection of MA methods and conditions was done on the basis of a literature survey (Suryanarayana, 2001; Mukhopadhyay et al., 1998; Cayron et al., 2004). Commercially pure elemental Fe, Cr, W, Ti and Y_2O_3 powders (more than 99.8% of purity) for the ODS ferritic steel with the composition of Fe-14Cr-2W-0.3Ti-0.3Y_2O_3 (in wt.%) were mechanically alloyed in a planetary ball mill equipped with stainless steel vials and balls, performed under argon or hydrogen atmosphere. Two different BPR's of: 10:1 and 20:1 (100 and 200 stainless steel balls with a diameter of 10 mm) and two different rotation speeds (RS) of 250 rpm and 350 rpm were used. At selected times a small amount of as-milled powder was taken out from the milling jar for further morphology and microstructure analyses. To minimize air contamination of the powder loading and unloading of the powder was performed in an argon glove box. The time of MA was optimized by studying the structural evolution of the powder by means of X-ray diffractometry (XRD), in a Siemens D5000 device, using the Cu-Kα radiation (λ=0.15406 nm). The crystallite mean size and lattice strain were determined by the Williamson-Hall method ($B_s \cos\theta = 2(\varepsilon)\sin\theta + k\lambda/D$) [8], where B_s is the full-width at half-maximum of the diffraction peak (FWHM), θ is the Bragg angle, ε is the internal lattice strain λ is the wavelength of the X-ray, D is the crystallite size and k is constant (k=0.9). B_s can be calculated from; $B^2_s = B^2_m - B^2_c$, where B_s is the peak broadening due to instrumental effect measured using crystallized LaB_6 standard and B_m is the eva-

luated width. MA process was conducted until the solute elements peaks in X-ray diffraction patterns disappeared.

The powders morphology and microstructure were studied using scanning electron microscopy (SEM) and transmission electron microscopy (TEM). The etched microstructure of the powder was observed by means of optical microscopy (OM). Chemical analysis of the powders was performed using wavelength dispersive X-ray fluorescence spectroscopy (WD-XRF) as well as LECO TC-436 and LECO IR-412 analysers for measurements of O, N and C contents, respectively.

After MA the ODS powders were submitted to hot isostatic pressing (HIP) at the temperature of 1150º C and pressure 200 MPa for 4 hours. Density of the specimens after compaction was measured by means of Archimedes method. Microhardness measurements were performed by using a Vickers diamond pyramid and applying a load of 0.98N for 15s. Each result is the average of at least 10 measurements.

3. RESULTS AND DISCUSSION

3.1. Morphology and microstructure of the ODS powders after MA

The particles of the as-received elemental ODS ferritic steel powders appear mostly round in shape, with an average size of about 10 µm (see Fig. 1a). SEM micrographs of the particles after MA for 50 h in a planetary ball mill with a BPR of 10:1 and RS of 250 rpm are shown in Fig. 1a. Fig 2 shows changes of the particles size during MA. At the early stage of ball milling fast increase in the particle size up to 150 µm were observed (see Fig. 2). Further milling, up to 8 h, leads to a significant decrease in the particle size and uniform size distribution. In prolonging the time of MA up to 12 h agglomeration process takes place again increasing the size of the particles from 10 to 80 µm. However, further prolongation of the milling time resulted in the hardening and fracturing of the particles due to fatigue failure mechanism. This trend, gradual refining of the powder, was observed up to 40 h of MA. From 40 to 50 h of MA a small variation of particle size can be observed probably due to the equilibrium state between fracturing and welding of the particles. Finally, after 50 h of MA, about 10 µm in diameter and homogenous particles were obtained.

It was also observed that by increasing the rotation speed from 250 to 350 rpm the milling time was reduced from 50 up to 42 h. When a BPR of 20:1 and a RS 350 rpm were applied the time of formation of a solid solution decreases up to 22 h. SEM observations of the elemental ODS powders (see Fig. 1) revealed that varying the milling parameters: BPR, RS or milling atmosphere (argon or hydrogen), no significant changes in the morphology of the ODS powders were achieved and about 10 µm in diameter particles were produced. However, a higher C content (about 20%) was detected in the powder using higher BPR of 20:1 and about 20% of oxygen content was reduced after using hydrogen atmosphere (see Table 1).

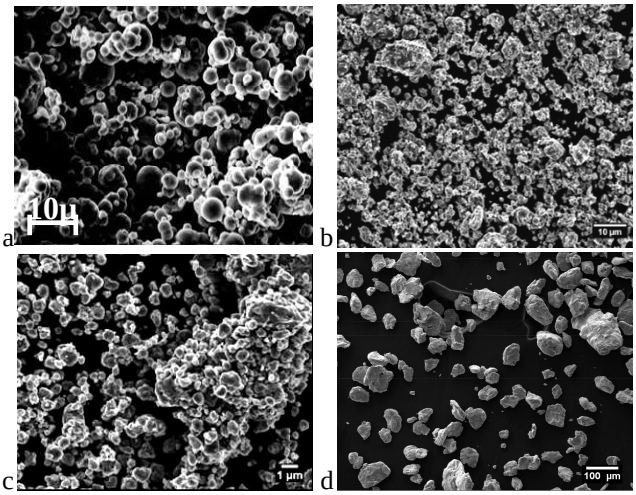

Fig. 1. Morphology of the ODS powder particles: a) as-received elemental powder, b) elemental powder MA for 50 h in argon, BPR 10:1, c) elemental powder MA for 22 h in argon, BPR 20:1, and d) pre-alloyed powder MA for 20 h in hydrogen, BPR 10:1

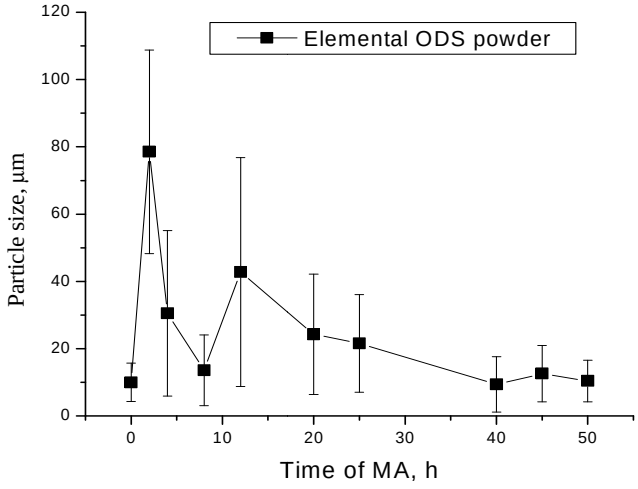

Fig. 2. Particle size distribution of the elemental ODS powder during MA in the planetary ball mill for 50 h in argon

Table 1. Chemical composition (in wt.%) of the ODS Fe-14Cr-2W-0.3Ti-0.3Y_2O_3 elemental and pre-alloyed powders after MA in the planetary ball mill

Chemical content, wt.%						
Conditions	C	Cr	W	Ti	Y	O
As-received	0.078	14.1	1.96	0.31	0.23	0.338
Elemental, MA in Ar for 50 h	0.088	13.7	1.84	0.26	0.21	0.482
Elemental, MA in H_2 for 42 h	0.067	13.7	1.80	0.25	0.28	0.372
Pre-alloyed, H_2, 20 h	0.043	13.5	1.92	0.33	0.25	0.175

It is well known that the MA technique yields contamination of the milled powder, which substantially alters the nature of the particles and therefore changes the final

properties of a bulk material (Mukhopadhyay et al., 1998; Ohtsuka et al., 2005). The data in Table 1 shown that the un-milled ODS powder contains a high oxygen content (0.338 wt.%) and after MA in a high purity argon atmosphere (99.9999 wt.%) an oxygen content of 0.482 wt.% was measured. The amounts of such elements as C, N, Mn and Si also increased due to the contamination coming from the grinding media.

To reduce oxygen and carbon content MA, a process with application of a pre-alloyed, gas-atomised Fe-14Cr-2W powder with 0.3%Y_2O_3 and 0.3%Ti was performed. The MA process was carried out up to 20 h under pure hydrogen atmosphere using BPR 10:1 and rotation speed 350 rpm. Fig. 1d shows SEM image of the pre-alloyed ODS powder after ball milling. According to the SEM observations the pre-alloyed powder, in comparison with the elemental one, exhibits more than 4 times larger particles with an average size of about 45µm, however, C and O content is significantly lower.

Optical micrographs of the etched elemental powder after MA for different milling times revealed that during the initial stage of milling (up to 10 hrs) a typical lamellar microstructure was observed (Fig 3a). Prolongation of the MA time caused refinement of the lamellas. Featureless contrasts as well as cracks that initiate break down of the particles are observed. After MA (Fig. 3b), the powder consists of a huge number of an agglomerated particles which form featureless image what may suggest that the particles exhibit nano-sized grains.

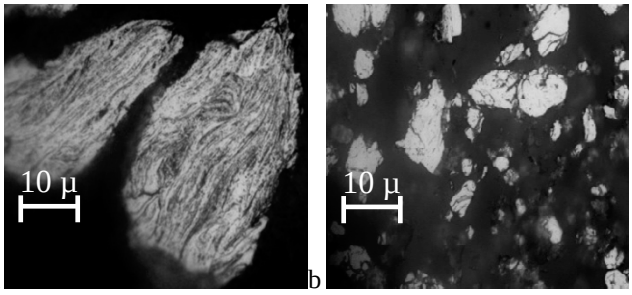

a b

Fig. 3. Microstructure of the elemental powder MA in argon for: a) 10 h and b) 50 h

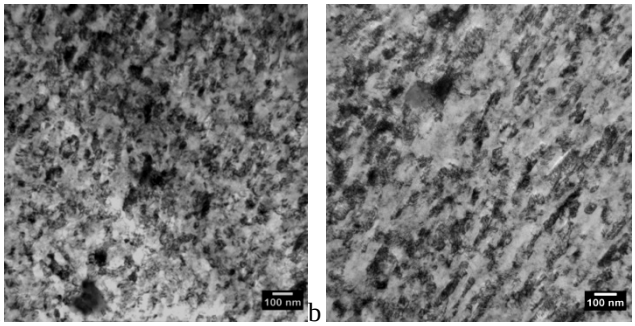

a b

Fig. 4. Bright-field TEM images of: a) elemental ODS powder MA in argon, and b) pre-alloyed ODS powder MA in hydrogen

Figs. 4a and 4b show TEM images of elemental and pre-alloyed ODS powders after mechanical alloying under argon and hydrogen atmosphere and using the same milling conditions (BPR=10:1, RS=350 rpm). TEM observations indicate that both powders have a strongly deformed and nano-sized microstructure and no yttria particles. However, some differences of the microstructure are also observed. The elemental powder has equiaxed nano-sized grains whereas elongated (textured) in the direction parallel to the surface of the particle grains are observed in the case of pre-alloyed powder. It can also be noticed that it was difficult to estimate the nano-grain size, due to the lack of clearly visible grain boundaries. Thus, results of the X-ray diffraction tests of the powders will be presented in the next section 3.2.

3.2. XRD analysis of the ODS powders

X-ray diffraction patterns of the ODS elemental and pre-alloyed powders MA in the planetary ball mill are shown in Figs. 5 and 6, respectively**.** After very short time of MA (2 h), in the case of elemental powder, the peaks of Y_2O_3 and the other solute elements disappeared completely and XRD pattern exhibits major α-Fe and W peaks (see Fig. 5). With increasing the milling time the intensity of Fe and W peaks decreases and its width increases due to a reduction of the crystallite size and increase in the deformation level of the particles. After 50 h of ball milling of the W peak disappears completely suggesting that MA process is accomplished.

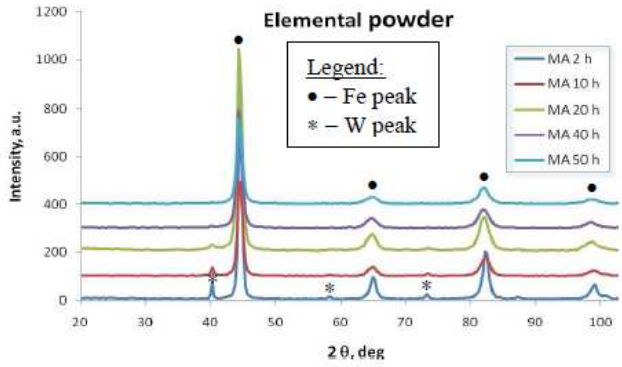

Fig. 5. XRD plots of the elemental powder MA in the planetary ball mill up to 50 h in argon

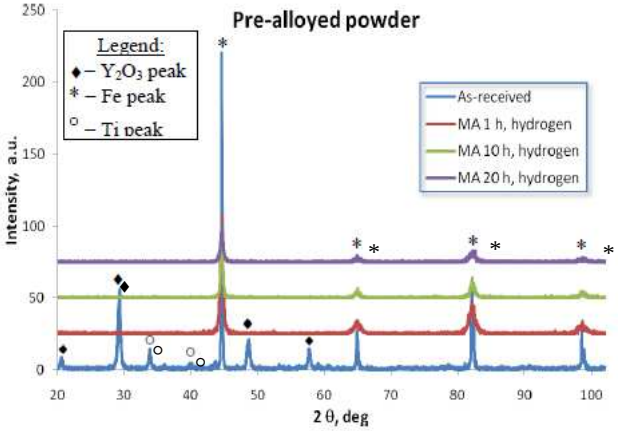

Fig. 6. XRD plots of the pre-alloyed powder MA in planetary ball mill up to 20 h in hydrogen

Also XRD examinations of the pre-alloyed powder (see Fig. 6) revealed that after 1 h of MA the peaks of Y_2O_3 and Ti disappeared what suggests that Y_2O_3 particles were completely dissolved in the ODS steel matrix. It seems highly probable, however, that yttria could still remain as a small particles incorporated deeper into the steel matrix, and as a consequence, could give a weaker X-ray signal than from the yttria particles lying on the surface of the ODS powder. This is due to the limited penetration depth of the X-rays into the material described in literature (Cullity, 1965). Hence, MA process of the pre-alloyed powder was continued up to 20 h to ensure homogenous incorporation of the Y_2O_3 particles in the ODS steel powder.

Detailed analysis of the XRD spectra indicates that during MA the main [110] α-Fe peak is gradually broadened and shifted towards lower 2θ angle values. This indicates an increase in solid solubility of the solute elements in the α-Fe matrix, an increase in the lattice strain as well as the gradual reduction of the crystallite size as it was confirmed in Figs. 7 and 8. In the early stage of MA a rapid decrease in the crystallite size to about 40 nm was observed (Fig. 7). Further ball milling proceeds relatively slowly and finally elemental and pre-alloyed powders reach an average crystallite size about 35 and 32 nm, respectively. These results are not consistent with TEM observations presented in Fig. 4. However, it is well known (Suryanarayana, 2001) that TEM reveals grain size images, whereas the X-ray technique gives information about an average crystallite size defined as coherently diffracted domain.

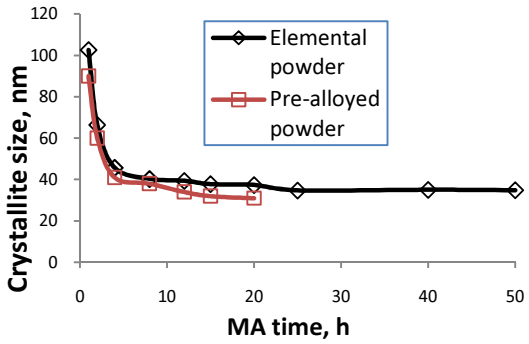

Fig. 7. Crystallite size plotted as a function of the milling time

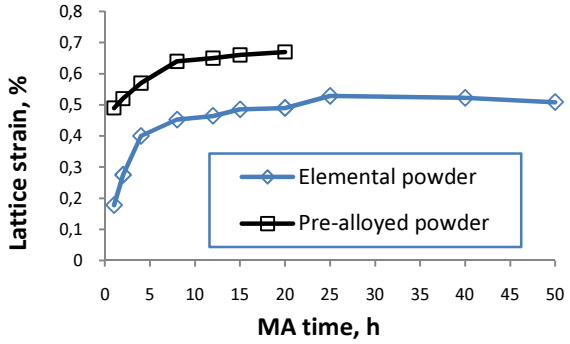

Fig. 8. Lattice strain vs. MA time of elemental and pre-alloyed powders

Fig. 8 shows the lattice strain value of the ODS powders, calculated from XRD data, and both milled using the same milling conditions. These results indicate that a higher about 30% lattice strain exhibits pre-alloyed powder.

This is probably due to an initial solid solution strengthening effect of the pre-alloyed powder. On the contrary, smaller and more reactive elemental powder particles may undergo faster recovery process, and as a consequence, a lower internal strain can be measured (Hwang, 2001). Nevertheless, both powders demonstrate similar trends, the lattice strain increase and crystallite size decrease with the milling time prolonging and after a certain period of milling a steady state is reached.

3.3. HIPping of the ODS powders

Following MA, the consolidation process was carried out under a pressure of 200 MPa at a temperature of 1150° C for 4 h. The results of microhardness and apparent density of the specimens after HIPping are summarized in Tab. 2.

The obtained in Table 2 results indicate that the highest density and microhardness value has the pre-alloyed powder mechanically alloyed in hydrogen. On the contrary, the lowest density has the material consolidated from elemental powder MA in argon. This is a consequence of the highest impurities content measured in the elemental powder after milling which can not be reduced during further degassing and HIPping process.

Tab. 2. Microhardness and density results of the ODS ferritic steel specimens after MA in different atmospheres and HIPped under a pressure of 200 MPa at 1150° C for 4 h

As-HIPped	Elemental, MA 42 h, argon	Elemental, MA 42 h, H_2	Pre-alloyed, MA 20 h, H_2
$\mu HV_{0.1}$	410±21	345±14	425±17
Apparent density, %	99.20*	99.52*	99.78*

** Apparent density=specimen density/theoretical density of an ODS ferritic steel (theoretical density=7.84 g/cm^3)*

These results also reveal that the parameters of HIPping process were suitable to produce almost fully dense ODS ferritic steel material.

4. CONCLUSIONS

On the basis of the results the following conclusions can be drawn:

1. There are significant differences in the morphology of the elemental and pre-alloyed powders after MA. About four times smaller particle were obtained after ball milling of the elemental powder whereas, larger and flakey-like particles were observed in the case of pre-alloyed powder.
2. An increase in the parameters of MA process yields a decrease in the time of milling, however, no significant changes in the morphology of particles have been observed.
3. The average crystallite size of about 35 nm, estimated from XRD spectra, was found comparable for both powders. However, in the case of pre-alloyed powder

TEM observations revealed elongated up to 100 nm nano-grains what is not in a good accordance with XRD results.

4. MA under argon atmosphere resulted in an increase of the O content which had detrimental influence on the density of the bulk material after HIPping.
5. It was found that the highest density and microhardness value was achieved when pre-alloyed powder was consolidated.

REFERENCES

1. **Benjamin J. S.** (1976), Mechanical Alloying, *Scientific American, 234, 40-8*.
2. **Cayron C. et al.** (2004), Microstructural evolution of Y_2O_3 and $MgAl_2O_4$ ODS EUROFER steels during their elaboration by mechanical milling and hot isostatic pressing, *Journal of Nuclear Material*, Vol. 335, 83-102.
3. **Chul-Jin Choi** (2000), Preparation of ultrafine TiC–Ni cermet powders by mechanical alloying, *Journal of Materials Processing Technology*, Vol. 104, 127-132.
4. **Cullity B. D.** (1965), *Elements of X-ray Diffraction*, *Addison-Wesley Publishing Company*, INC. London, England.
5. **Hwang S., Nishimura C., McCormick P. G.** (2001), Mechanical Milling of Magnesium Powder, *Material Science and Engineering*, Vol. A318, 22-33.
6. **Mukhopadhyay D. K., Froes F. H., Gelles D.S.** (1998), Development of oxide dispersion strengthened ferritic steels for fusion, *Journal of Nuclear Materials*, Vol. 258-263, 1209-1215.
7. **Ohtsuka S., et al.** (2005), Nano-structure control in ODS martensitic steels by means of selecting titanium and oxygen contents, *Journal of Physics and Chemistry of Solids*, Vol. 66, 571-575.
8. **Patil U., et al.** (2005), An unusual phase transformation during mechanical alloying of an Fe-based bulk metallic, *Journal of Alloy and Compounds*, Vol. 389, 121-126.
9. **Suryanarayana C.** (2001), Mechanical alloying and milling, *Progress in Mat. Science*, Vol. 46, 1-184.
10. **Williamson G .K., Hall W. H.** (1953), X-ray line broadening from filed aluminum and wolfram, *Acta Metall.*, Vol.1, p. 22.

This work was supported by Bialystok Technical University, a grant no. W/WM/21/10.